RSC Advances

PAPER

View Article Online
View Journal | View Issue

Cite this: *RSC Adv.*, 2024, **14**, 13926

Mechanistic explanation and influence of molecular structure on chemical degradation and toxicity reduction by hydroxyl radicals†

You-Yi Lee, Hao-Chien Cheng and Chihhao Fan *

This study explored the influence of structural characteristics of organic contaminants on the degradation during an advanced oxidation process (AOP). The target contaminants were acetaminophen (ACT), bisphenol A (BPA), and tetracycline (TC). The Fenton process was selected as the model process in which major reactive species of hydroxyl radicals in most AOPs are generated for target compound degradation. The optimal reagent concentration ratio was $[Fe^{2+}]/[H_2O_2]$ = 0.5 mM/0.5 mM in an acidic condition, resulting in 83.49%, 79.01%, and 91.37% removals of ACT, BPA, and TC, respectively. Contrarily, the mineralization rates were apparently lower compared to their respective removal efficiencies. Experimental observation also suggested that the aromatic structure was rather difficult to degrade since their unsaturated electron clouds would hinder the attack of hydroxyl radicals due to electric repulsion. The preferred attacking sites of an aromatic ring differ due to the functional groups and structure symmetry. However, the electrophilic attack of the hydroxyl radical is the major reaction for decomposing aliphatic structures of cyclic or branched organics, resulting in the highest removal and mineralization of TC among these three tested chemicals. In addition, an apparent removal of a contaminant may not necessarily reduce its toxic impact on the environment.

Received 1st February 2024
Accepted 20th April 2024

DOI: 10.1039/d4ra00827h

rsc.li/rsc-advances

Introduction

Emerging contaminants are chemical pollutants that are "newly or not previously recognized", "not regulated by legislation" and "risky to human health and the environment", which include, but are not limited to, medicines, pharmaceuticals, personal care products (PPCPs), endocrine-disrupting chemicals (EDCs), and industrial additives. They are often toxic to living beings and pose adverse effects on biological metabolism, and cannot be effectively removed by conventional wastewater treatment plants.[1] Some emerging contaminants have been found to function similarly to hormones that affect the immune, nervous, and endocrine systems, thus causing negative impacts (*e.g.*, disrupting the sexual development and reproductive cycles) on organisms with prolonged exposure.[2–7] It is often recommended that the types, sources, transport, and fate of emerging contaminants should be investigated to assess their impacts on the environment.[8–11]

Methods to remove such organic compounds from water have been explored, including adsorption, flocculation,[12] chemical precipitation, microbial degradation,[13,14] and AOPs.[15] Among these possible treatment technologies, AOPs have gained increasing attention because of their ability to degrade most organic pollutants into smaller fractions or form carbon dioxide through mineralization.[16] For example, acetaminophen (ACT), bisphenol A (BPA), and tetracycline (TC) have been treated by physical adsorption, biological oxidation, or chemical oxidation.[17–20] However, the absorbed contaminants usually require further treatment to decrease their toxicity, and biological oxidation might not be as effective as expected. Against this background, AOP has been regarded as an alternative to treat emerging contaminants.

Various oxidants and catalysts have been found capable of producing radicals with strong oxidation power. Generally, the often-used radicals include the hydroxyl radical (˙OH), sulfate radical ($SO_4^{\cdot-}$), and chlorine radicals (Cl˙), all of which have high redox potentials to decompose organic contaminants.[2,21–23] Among them, the ˙OH is the mostly-applied oxidant[24,25] that has been observed in the AOP systems containing hydrogen peroxide, persulfate, and chlorine. Besides the applied dose of the oxidants, the chemical structure of the target compound also affects the AOP effectiveness significantly. Despite the above statement, little study has been reported regarding the influence of participating molecular structure on AOP treatment efficiency.

Along this context, this study aimed to explore the influence of structural variation of target organics on the AOP degradation efficiency. The Fenton process was selected since it is the classic mechanism of ˙OH generation. The degradation experiments

Department of Bioenvironmental Systems Engineering, National Taiwan University, Taiwan. E-mail: chfan@ntu.edu.tw

† Electronic supplementary information (ESI) available. See DOI: https://doi.org/10.1039/d4ra00827h

were carried out under acidic conditions, which is a favorable environment for the Fenton process. Three emerging contaminants ACT (a common painkiller), BPA (commonly found in plastic products), and TC (a widely-used antibiotic) were selected as the target compounds that exhibit various chemical structures of aromatic, cyclic, and aliphatic functionalities.

Materials and methods

Chemicals and reagents

Reagent-grade (99% purity or above) ACT, BPA, and TC (properties summarized in Table 1), hydrogen peroxide, phosphoric acid, sodium persulfate solution, and sodium thiosulfate were obtained from Sigma-Aldrich. Ferrous sulfate was purchased from Avantor, and methanol and oxalic acid were procured from Honeywell. Sulfuric acid (H_2SO_4) and phosphate buffer were used to adjust the pH, and $Na_2S_2O_3$ was used to quench the Fenton reaction. Methanol and oxalic acid were employed as the mobile phase for high-performance liquid chromatography (HPLC) analysis.

Fenton experiment procedure

All the Fenton degradation experiments were conducted in a 1000 mL beaker under ambient temperature (25–30 °C). H_2SO_4 was added to maintain the pH at 3 for the Fenton degradation.[26] The concentrations of the ferrous ions (Fe^{2+}) and H_2O_2 varied from 0.1–0.5 mM at the $[Fe^{2+}]/[H_2O_2]$ ratio of 1 : 1 to determine the optimal dose of Fe^{2+} and H_2O_2 to achieve the highest degradation efficiency. Experiments by maintaining a constant Fe^{2+} concentration at 0.5 mM and varying the concentration of H_2O_2 (0.1, 0.3, 0.5 mM) were conducted to explore the effect of the structural variation on the degradation efficiency. An aliquot of aqueous sample was collected at 0, 0.5, 1, 2, 5, 10, 15, and 30 min after the initiation of the Fenton reaction and immediately quenched by $Na_2S_2O_3$ before passing through a 0.22 μm filter. The concentrations of ACT, BPA, and TC were quantified by HPLC to calculate the degradation efficiency. The total organic carbon (TOC) of each collected sample was analyzed to determine the degree of mineralization.

Analytical methods

The HPLC employed was a Thermo Scientific Ultimate 3000 HPLC system equipped with a Thermo Scientific Acclaim 120 C18 5 μm 120 A (4.6 × 250 mm) column. The UV wavelengths at 249, 280, and 360 nm were used for detecting ACT, BPA, and TC, respectively. The column temperature was maintained at 30 °C. The injection volume of acetaminophen was 20 mL and the flow rate was 0.2 mL min^{-1}, with a mobile phase of methanol and deionized (DI) water (methanol : DI water = 20 : 80). The injection volume of BPA was 20 mL and the flow rate was 0.5 mL min^{-1} with methanol : DI water (30 : 70) as the mobile phase. The injection volume of tetracycline was 20 mL and the flow rate was 1.7 mL min^{-1}, with a mobile phase of methanol and oxalic acid (0.01 M). The gradient conditions (methanol : oxalic acid) were as follows: 15 : 85 at 0 min, 30 : 70 at 4 min, 50 : 50 at 5 min, 75 : 25 at 6 min, 50 : 50 at 8 min, 30 : 70 at 9 min, and 15 : 85 at 11 min. Total organic carbon (TOC) analysis was performed using a TOC analyzer (TOC-OIA_1030W) which employed a low-temperature wet oxidation method. An acidifier (5% phosphoric acid solution) was added to remove the inorganic carbon and the oxidizer (100 g L^{-1} sodium persulfate solution) was introduced at 100 °C to oxidize the organic matter into CO_2 which was transferred into a non-dispersive infrared analyzer that can absorb a specific wavelength by the carrier gas (oxygen).

Risk analysis methodology

The toxicity of ACT, BPA, TC, and their possible degradation products were predicted using ECOSAR (Ecological Structure Activity Relationship Class Program) which is one of the modules in EPI (Estimation Programs Interface) Suite™ (version 4.11) released by the US Environmental Protection Agency (EPA). The ECOSAR estimates the acute and chronic toxicity to aquatic organisms, including fish, invertebrates, and

Table 1 Chemical and physical properties of ACT, BPA, and TC

Chemical name	Structural formula	Molecular formula	Molecular weight	Water solubility	Melting point (°C)
Acetaminophen	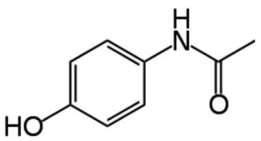	$C_8H_9NO_2$	151.16 g $mole^{-1}$	12.78 g L^{-1}	169
Bisphenol A	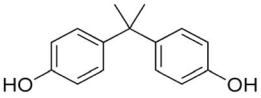	$C_{15}H_{16}O_2$	228.29 g $mole^{-1}$	120 mg L^{-1}	158
Tetracycline	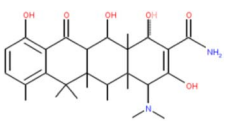	$C_{22}H_{24}N_2O_8$	444.44 g $mole^{-1}$	231 mg L^{-1}	170

green algae. In this study, the median lethal concentration (LC_{50}) was estimated by ECOSAR to compare the toxicity between the parent compound and its degradation products, assessing the ecological risk during the degradation of each parent compound.

Theoretical assessment of potential reactive sites by Fukui function

The Fukui function is useful to predict the electrophilic, nucleophilic, and free radical attack sites in a compound, which is defined as:

$$f(\vec{r}) = \left[\frac{\partial \rho(\vec{r})}{\partial N}\right]_v \quad (1)$$

where $\rho(\vec{r})$ is the electron density at point r in space, N is the number of electrons, and v is the external potential. In the condensed Fukui function (CFF), the reactive sites have larger values than other regions, which makes the potential preferred reaction sites predictable. Three types of condensed Fukui indices, which are f^+, f^-, and f^0, represent nucleophilic attack, electrophilic attack, and radical attack, respectively. The calculation of reactions:

$$\text{Nucleophilic attack: } f^+ = [q_i(N+1) - q_i(N)] \quad (2)$$

$$\text{Electrophilic attack: } f^- = [q_i(N) - q_i(N-1)] \quad (3)$$

$$\text{Radical attack: } f^0 = \left[\frac{q_i(N-1) - q_i(N+1)}{2}\right] \quad (4)$$

where q_i is the atomic charge.

Density functional theory (DFT) calculations for the Fukui function were carried out by Gaussian 09 program software. For ACT and BPA, 6-31G(d,p) and B3LYP (Becke's three parameters and Lee–Yang–Parr functional) were utilized as a basis set. For TC, 6-311+g(d,p) and functional M06-2X-D3 were the basis sets used for C, H, O, and N. Multiwfn software was used to calculate and visualize the condensed Fukui indices.

Results and discussion

The degradation by hydroxyl radicals

The degradation efficiencies of ACT, BPA, and TC at the 1 : 1 ratio of $[H_2O_2]:[Fe^{2+}]$ are presented in Fig. 1, showing that the degradation occurred rapidly within 5 to 10 minutes and remained stable thereafter as the H_2O_2 concentration increased from 0.1 mM to 0.5 mM. The maximum removal of ACT, BPA, and TC was 83.49%, 79.01%, and 91.37%, respectively, with 0.5 mM Fe^{2+}/0.5 mM H_2O_2, consistent with the findings in the literature.[27–29] With the same oxidant/catalyst dose application, different removal rates were observed, implying that the molecular structure should be a factor that affects the compound degradation. In the experiment with 0.1 mM applied reagent doses, TC showed the highest removal (76.95%) rate among the three investigated chemicals.

Structurally speaking, BPA consists of two aromatic rings, ACT consists of one aromatic ring, and TC consists of one aromatic ring along with three additional cyclic rings. Molecular structures with higher aromaticity decreased the removal efficiency in an AOP. The aromatic ring is a resonance structure that is more stable than the saturated and unsaturated covalent bonds of the cyclic structure (as present in TC) and difficult to degrade. It has also been suggested that the AOP degradation efficiency would be reduced with the increase in ring functional groups.[30]

The degradation curve of emerging contaminants by $^{\bullet}OH$ could be described by the first-order kinetic model (eqn (5)),[31] where C_0 and C_{equil} are the initial and equilibrium concentrations of the target compound, and k is the rate constant in minutes.

$$C = (C_0 - C_{equil}) \times e^{-kt} + C_{equil} \quad (5)$$

The kinetic parameters are summarized in Table 2. The reaction between H_2O_2 and Fe^{2+} produces $^{\bullet}OH$ that achieves an obvious removal of the target contaminants. The degradation efficiency by $^{\bullet}OH$ was positively correlated to the Fe^{2+} and H_2O_2 concentrations. However, the degradation rate is not proportional to the applied reagent concentrations, because of the complicated reacting mechanism in the Fenton process.

The decomposition effect of various oxidant concentrations

The result of using 0.5 mM Fe^{2+} concentration (*i.e.*, catalyst in the process) and varying H_2O_2 concentrations (*i.e.*, 0.1, 0.3, and 0.5 mM as the oxidant) are shown in Fig. 2A, C and E, indicating that the degradation was enhanced with increasing H_2O_2 concentration, with TC being the most-degraded and BPA the least-degraded target compounds. The degradation is regressed by a first-order kinetic model and the kinetics parameters are shown in Table S1.†

The TOC content was measured for mineralization assessment and the results are shown in Fig. 2B, D and F. For the investigated contaminants, the mineralization was improved as the H_2O_2 concentration increased from 0.1 to 0.5 mM. The TC was found to have higher mineralization rates compared to ACT and BPA. Overall, the mineralization rates remained relatively low compared to the removal rates.

In an $^{\bullet}OH$-driven AOP, the target compound decomposes to form intermediates/fractions, which may become scavengers or competitive organics of available $^{\bullet}OH$.[32,33] Therefore, the unreacted contaminants and resulting intermediates/fractions would compete for $^{\bullet}OH$ to achieve further decomposition. In the present study, the parent contaminant remains rather difficult to decompose because of the aromatic structure, as opposed to the resulting intermediates and fragmented molecules. Also, the amount of parent contaminants was outnumbered by that of the resulting intermediates after the initiation of the degradation process. From the classical collision theory of chemical reactions and considering the aromaticity of tested parent compounds, the $^{\bullet}OH$ would react with intermediates preferably, and no apparent increase in contaminant removal was observed.

From the above statements, the apparent removal of tested contaminants suggested that their molecular structures have been altered, either by bond-breaking in the aliphatic and

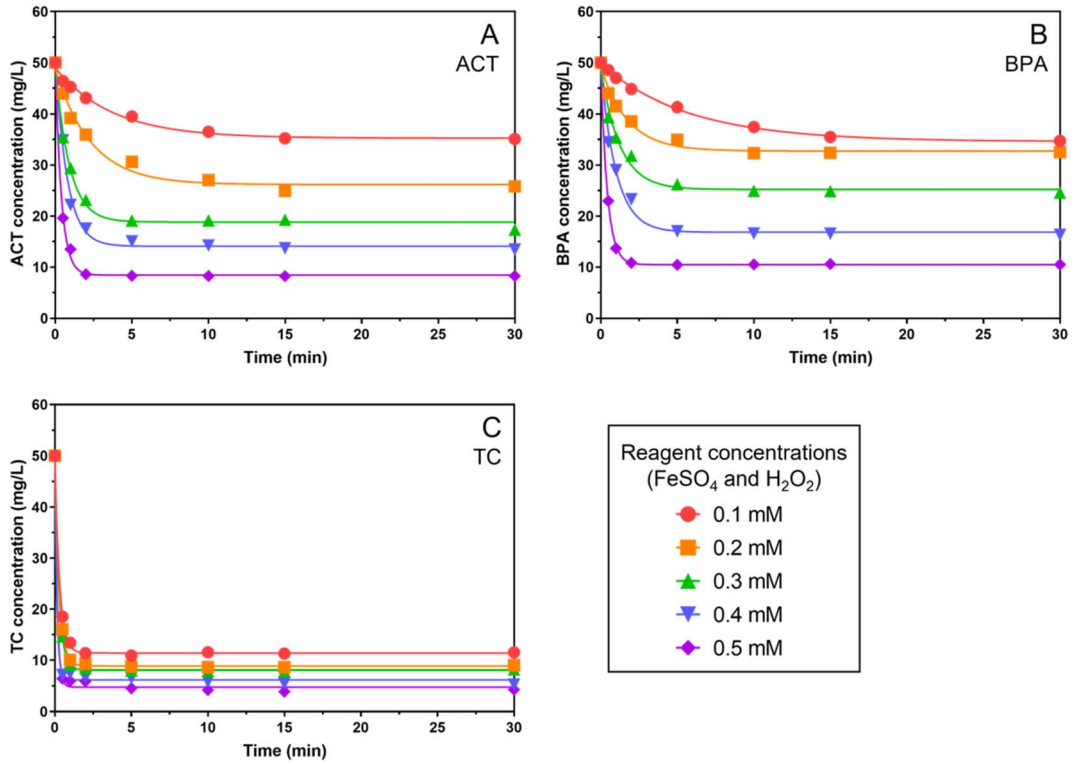

Fig. 1 The degradation of the ACT (A), BPA (B), and TC (C) by the hydroxyl radical at different concentrations of $[Fe^{2+}]$: $[H_2O_2]$ with the ratio of 1 : 1. The degradation curves are simulated by first-order kinetics.

Table 2 Kinetic parameters for Fenton oxidation of ACT, BPA, and TC at different concentrations of $[Fe^{2+}]$: $[H_2O_2]$ and maintaining a ratio of 1 : 1[a]

Compound	Reagent concentration (mM)	C_0	C_{equil}	k (min^{-1})	R^2
ACT	0.1	48.95	35.26	0.2669	0.9877
	0.2	48.81	26.17	0.4313	0.9831
	0.3	49.58	18.82	1.1000	0.9946
	0.4	50.38	14.07	1.2810	0.9929
	0.5	49.87	8.42	2.4640	0.9977
BPA	0.1	49.71	34.60	0.1731	0.9976
	0.2	49.14	32.74	0.5673	0.9849
	0.3	49.01	25.21	0.8062	0.9853
	0.4	49.10	16.82	0.9897	0.9907
	0.5	50.05	10.46	2.3610	0.9997
TC	0.1	49.98	11.41	3.3110	0.9994
	0.2	50.00	8.89	3.4970	0.9998
	0.3	50.00	8.12	3.7160	0.9998
	0.4	50.00	6.21	7.6310	0.9980
	0.5	50.00	4.80	6.5000	0.9978

[a] C_0 is the initial concentration of the target compound at 0 min; C_{equil} is the target compound concentration when achieving Fenton equilibrium; k is the first-order kinetic rate constant; R^2 indicates the goodness of kinetic model fitting.

branched structures or by aromatic ring cleavage. The undecomposed parent compounds and the resulting organic fractions remain in existence during the degradation, supporting the observation that the degree of mineralization might be quite limited. Since $^{\bullet}OH$ is highly active and could be consumed rapidly as the bond-breaking process proceeds in the degradation, much more hydroxyl radicals (*i.e.*, more H_2O_2) are required to oxidize the existing target compounds and intermediate organics to increase the mineralization rate in the present study.

The toxicity variation evaluation in the degradation process using ECOSAR

Generally, water pollution control practice aims to remove aqueous pollutants through treatment processes and the efficiency is determined by the concentration difference of the target pollutant between influent and effluent wastewaters. While the issues of public and environmental health attract increasing attention, the potential threats from all the existing organics should be considered. In light of this concept, this study also evaluated the toxicity variation of a given target compound considering the toxic impact from the parent compound and its daughter intermediates during the degradation process. The pollutants' toxicities were assessed using the ECOSAR of EPI Suite software and the degradation pathways of ACT,[34] BPA,[20] and TC[35] were adopted from the literature. The structural parameters of the parent contaminants and the resulting intermediates were introduced into the EPI Suite and their 50% lethal concentrations (LC_{50}) were simulated using ECOSAR to establish the baseline toxicities of the target contaminants to fish (Fig. 3).

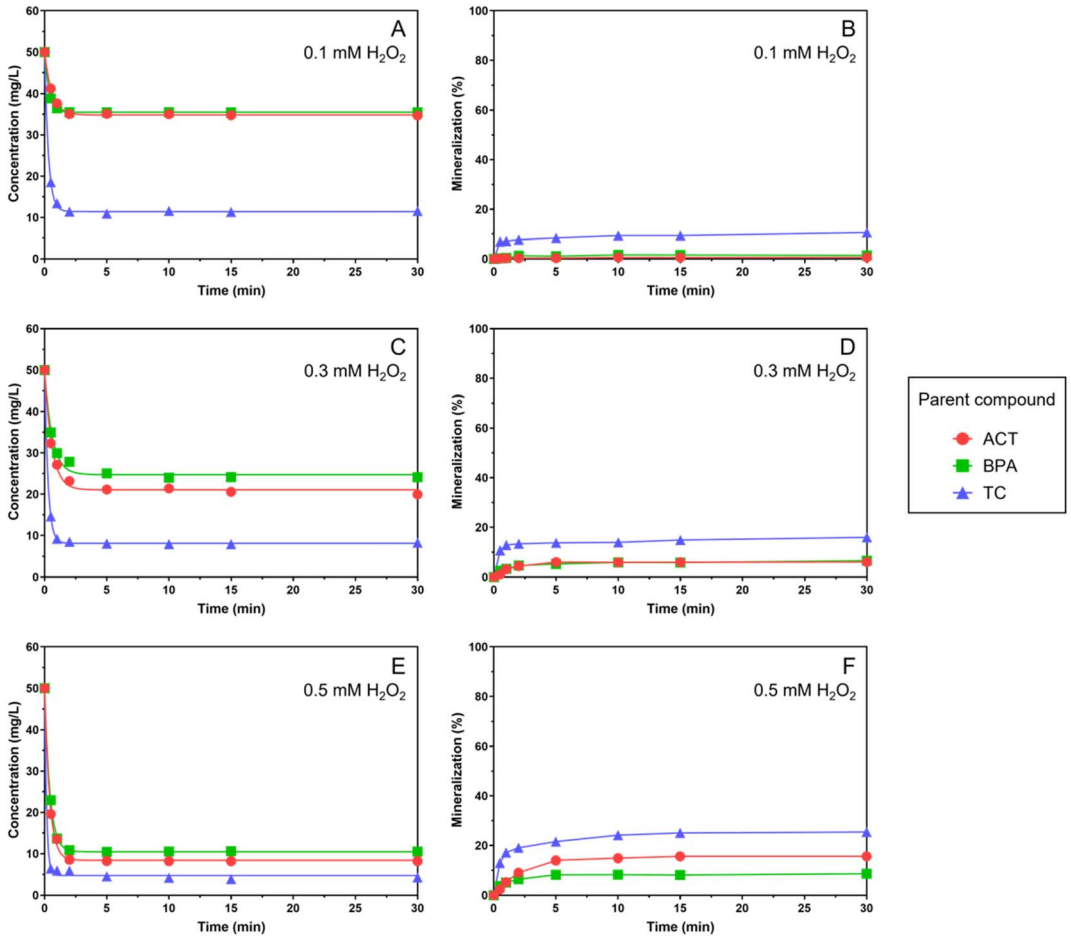

Fig. 2 The degradation (A), (C) and (E) and mineralization (B), (D) and (F) of the different contaminants at ferrous ion concentration of 0.5 mM and varying concentrations of H_2O_2. The degradation curves are simulated by first-order kinetics.

As shown in Fig. 3A, the resulting intermediates (other than organic acids and ammonium ion) during the degradation were found more toxic than ACT, implying that the overall chemical toxicity during AOP might increase if ultimate mineralization is not achieved. Theoretically, the intermediates may continue to oxidize, forming the end products of CO_2 and H_2O if enough $^{\cdot}OH$ are present. However, no reported studies have shown the full spectrum of possible oxidation by-products before mineralization for the investigated contaminants. Similar to the degradation of ACT, according to the pathway shown in Fig. 3C, all the proposed intermediates were considered more toxic than TC. Therefore, it is suggested that complete mineralization would be deemed appropriate if ACT or TC is treated with AOPs.

In contrast, the lethal concentrations of the observed intermediates (as shown in Fig. 3B) from BPA degradation increased, showing less toxicity of the resulting intermediates. In field practice, using AOPs to treat BPA seems to be a feasible alternative since the formation of intermediates would not increase the overall toxicity while complete mineralization is hardly achieved.

Based on a common perception of oxidation capability, AOPs were often used to treat recalcitrant organic contaminants since the oxidative radicals are highly reactive almost without selectivity. However, mineralization rates by AOPs are usually low, since complete breakage of all the organic bonds requires massive amounts of oxidants (*i.e.*, generated radicals in an AOP). The findings from the study showed that the existence of remaining intermediates may pose even higher threats to the ecology and environment. Therefore, a further evaluation of the suitability of the AOP application (*i.e.*, ecological risk analysis in addition to general treatment efficiency) should be conducted before its on-site practice.

Effect of the molecular structure on degradation by $^{\cdot}OH$

Among the three investigated chemicals, both ACT and BPA have a relatively simple structure (as shown in Table 1), and the number of aromatic rings in the structure affects the degradation rates. On the other hand, TC has one aromatic ring attached by three cyclic structures and branches and $^{\cdot}OH$ would attack the single-bonded structures preferentially.

In AOPs, decomposition by oxidants such as hydroxyl radicals, sulfate radicals, and superoxide radicals are the dominant oxidation pathways.[36] From the perspective of molecular structure, the radicals prefer to attack the highest occupied molecular orbital (HOMO) site on the target compound, which makes

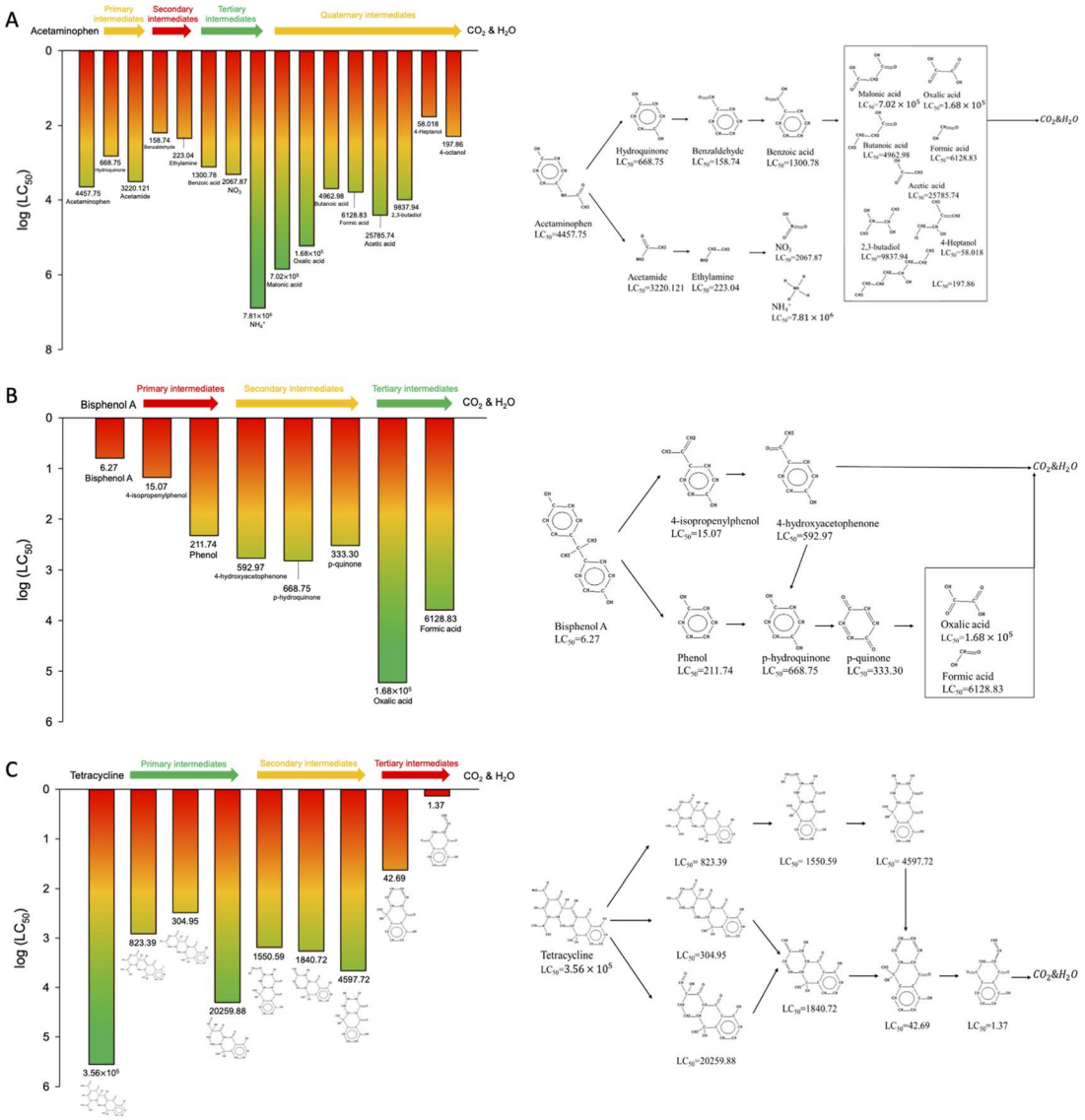

Fig. 3 The main toxicity variation and degradation pathway[20,34,35] of (A) ACT, (B) BPA, and (C) TC during the degradation process.

the radical-attacked preferred sites predictable. The Fukui index representing electrophilic attack (f^-) and radical attack (f^0) are considered based on the density functional theory (DFT).[37–39] Considering the primary reactive radical (*i.e.*, ˙OH) in the present study, the calculations of the Fukui index and the values were adopted from the literature and summarized in Tables S2–S4† and the possible reactive sites with ˙OH were shown in Fig. 4.[36,40–42]

For ACT containing a single benzene ring, the radicals prefer to attack the *para*-position of the benzene ring, opposite to the phenol group (*i.e.*, C6 position in Fig. 4A), and release hydroquinone and acetamide as degradation byproducts[36] (Fig. 3A). A similar radical attack on *para*-position was also shown at the formation of *p*-hydroquinone from phenol in the BPA degradation pathway (Fig. 3B). Different from ACT, BPA encompasses two benzene rings in a symmetrical structure, resulting in a barrier for ˙OH attack on the *para*-position of the phenol group. Instead, ˙OH is suggested to attack the *ortho*-position (*i.e.*, C1, C3, C12, C14 positions in Fig. 4B) of the phenol group of the benzene ring through hydroxylation.[41,42] Furthermore, phenol and 4-isopropenylphenol were formed *via* the β-scission (*i.e.*, cleavage of C–C bond) by the attack of ˙OH at C7 position (Fig. 3B).[20] In TC, both the most preferred radical and electrophilic attack site (highest f^0 and f^- value) is N19 position, forming a C–OH bond on C12. Subsequently, the C9–C12 covalent bond of the intermediate was broken by ˙OH attack, resulting in the cyclic cleavage of the IV ring (Fig. 3C).[40,43]

Compared to ACT and BPA, TC consists of both benzene and cyclic rings in its molecular structure and the ˙OH tends to degrade the non-aromatic part (*e.g.* side branches and cyclic ring) of TC first, thus explaining the highest overall degradation among the three target compounds. The highest f^0 value of TC appears at the side amine branch on the non-aromatic ring (*i.e.*, N19 position), leading to the fast first-step degradation of

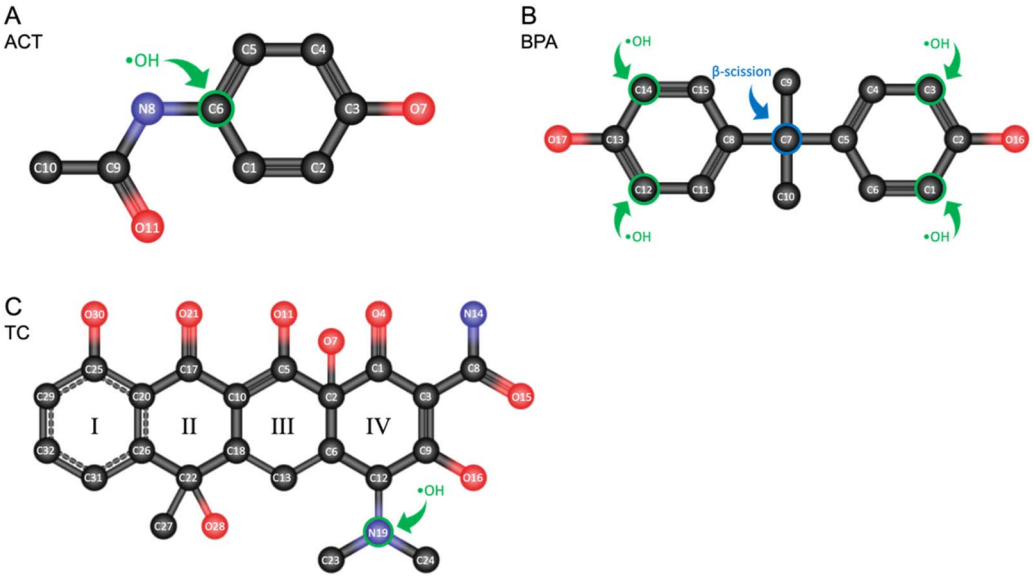

Fig. 4 The possible reactive sites with •OH predicted by Fukui index (f^- and f^0). (A) ACT, (B) BPA, and (C) TC.

parent compounds. Moreover, TC has a larger molecular size than ACT and BPA which increases the opportunity for collision reactions with free radicals, showing the highest apparent degradation rate (*i.e.*, the highest k value in Table S1†). For the actual degradation in the whole system including the intermediates, the Fukui function calculation can be applied to each intermediate to predict the preferred sites. The stable degradation was observed after 10 minutes because of the generated molecular fractions from parent contaminants by •OH reactions (Fig. 1 and 2).

Conclusions

In summary, this study explored the impact of molecular structure on the degradation efficiency by AOP and the overall toxicity in the degradation was assessed. The best operation condition occurred at 0.5 mM Fe^{2+} and 0.5 mM H_2O_2, resulting in the best removal rates of 83.49% for ACT, 79.01% for BPA, and 91.37% for TC in an acidic condition. Despite the occurrence of apparent removal, the mineralization rates were still low, implying the possible roles of reaction intermediates as the radical scavengers at the end of the AOP degradation. Also, the number of aromatic rings in the reactant is a critical factor impacting the degradation efficiency since the unsaturated aromatic electron clouds would hinder the possible attack by the •OH. On the contrary, non-aromatic branched structures would exhibit more vulnerability to the attack by •OH, resulting in a higher observed degradation efficiency. Among the three tested compounds, the most radical-attack preferred site with the highest f^0 value of TC is the side amine branch on the non-aromatic ring, causing the easiest decomposition of TC by hydroxyl radicals and showing the most obviously apparent degradation result. In addition, an apparent removal of a contaminant may not necessarily reduce its toxic impact on the environment. The reaction intermediates may possess higher toxicity than their parent compounds, implying that the AOP application may induce a higher overall toxicity to the ecology and environment.

Conflicts of interest

The authors declare no competing financial interest.

Acknowledgements

This work is partially supported by the National Science and Technology Council, Taiwan under the grant numbers of NSTC 108-2313-B-002-026 and 109-2313-B-002-049-MY2.

References

1 L. Mandaric, M. Celic, R. Marcé and M. Petrovic, in *Emerging Contaminants in River Ecosystems*, Springer, 2015, pp. 3–25.
2 M. Adeel, X. Song, Y. Wang, D. Francis and Y. Yang, *Environ. Int.*, 2017, **99**, 107–119.
3 L. Ma and S. R. Yates, *Sci. Total Environ.*, 2018, **640**, 529–542.
4 W. B. Whitman, *Cell Chem. Biol.*, 2017, **24**, 652–653.
5 R. Baccar, M. Sarrà, J. Bouzid, M. Feki and P. Blánquez, *Chem. Eng. J.*, 2012, **211–212**, 310–317.
6 E. J. Marti and J. R. Batista, *Sci. Total Environ.*, 2014, **470**, 1056–1067.
7 S. Sauvé and M. Desrosiers, *Chem. Cent. J.*, 2014, **8**, 15.
8 R. M. Clarke and E. Cummins, *Hum. Ecol. Risk Assess.*, 2015, **21**, 492–513.
9 M. Grassi, G. Kaykioglu, V. Belgiorno and G. Lofrano, in *Emerging Compounds Removal from Wastewater*, Springer, 2012, pp. 15–37.
10 S. Smith, *Philos. Trans. R. Soc., A*, 2009, **367**, 4005–4041.
11 J. Wilkinson, P. S. Hooda, J. Barker, S. Barton and J. Swinden, *Environ. Pollut.*, 2017, **231**, 954–970.

12 C. S. Lee, J. Robinson and M. F. Chong, *Process Saf. Environ. Prot.*, 2014, **92**, 489–508.
13 J. Liu and S. Mejia Avendaño, *Environ. Int.*, 2013, **61**, 98–114.
14 M. Sudha, A. Saranya, G. Selvakumar and N. Sivakumar, *Int. J. Curr. Microbiol. Appl. Sci.*, 2014, **3**, 670–690.
15 X. Hu, B. Liu, Y. Deng, H. Chen, S. Luo, C. Sun, P. Yang and S. Yang, *Appl. Catal., B*, 2011, **107**, 274–283.
16 A. Stasinakis, *Global NEST J.*, 2008, **10**, 376–385.
17 H. Katsumata, S. Kawabe, S. Kaneco, T. Suzuki and K. Ohta, *J. Photochem. Photobiol., A*, 2004, **162**, 297–305.
18 M. Umar, F. Roddick, L. Fan and H. A. Aziz, *Chemosphere*, 2013, **90**, 2197–2207.
19 L. Xu, H. Zhang, P. Xiong, Q. Zhu, C. Liao and G. Jiang, *Sci. Total Environ.*, 2020, 141975.
20 X. Zhang, Y. Ding, H. Tang, X. Han, L. Zhu and N. Wang, *Chem. Eng. J.*, 2014, **236**, 251–262.
21 A. Boscolo Boscoletto, F. Gottardi, L. Milan, P. Pannocchia, V. Tartari, M. Tavan, R. Amadelli, A. De Battisti, A. Barbieri, D. Patracchini and G. Battaglin, *J. Appl. Electrochem.*, 1994, **24**, 1052–1058.
22 C. Casado, J. Moreno-SanSegundo, I. De la Obra, B. Esteban García, J. A. Sánchez Pérez and J. Marugán, *Chem. Eng. J.*, 2021, **403**, 126335.
23 Y. Deng and R. Zhao, *Curr. Pollut. Rep.*, 2015, **1**, 167–176.
24 C. Fan, L. Tsui and M.-C. Liao, *Chemosphere*, 2011, **82**, 229–236.
25 N. Klamerth, S. Malato, M. Maldonado, A. Aguera and A. Fernández-Alba, *Environ. Sci. Technol.*, 2010, **44**, 1792–1798.
26 Y. S. Jung, W. T. Lim, J. Y. Park and Y. H. Kim, *Environ. Technol.*, 2009, **30**, 183–190.
27 W. Chen, C. Zou, Y. Liu and X. Li, *J. Ind. Eng. Chem.*, 2017, **56**, 428–434.
28 M. D. G. de Luna, M. L. Veciana, J. I. Colades, C.-C. Su and M.-C. Lu, *J. Taiwan Inst. Chem. Eng.*, 2014, **45**, 565–570.
29 M. H. Mahdi, T. J. Mohammed and J. A. Al-Najar, *Eng. Technol. J.*, 2021, **39**, 260–267.
30 M. A. Engwall, J. J. Pignatello and D. Grasso, *Water Res.*, 1999, **33**, 1151–1158.
31 D. Bhangare, N. Rajput, T. Jadav, A. K. Sahu, R. K. Tekade and P. Sengupta, *J. Anal. Sci. Technol.*, 2022, **13**, 7.
32 S. Gligorovski, R. Strekowski, S. Barbati and D. Vione, *Chem. Rev.*, 2015, **115**, 13051–13092.
33 Y.-Y. Lee and C. Fan, *Chemosphere*, 2020, **258**, 127338.
34 M. D. G. de Luna, M. L. Veciana, C.-C. Su and M.-C. Lu, *J. Hazard. Mater.*, 2012, **217**, 200–207.
35 Z. Zhu, X. Tang, S. Kang, P. Huo, M. Song, W. Shi, Z. Lu and Y. Yan, *J. Phys. Chem. C*, 2016, **120**, 27250–27258.
36 M. Qutob, M. A. Hussein, K. A. Alamry and M. Rafatullah, *RSC Adv.*, 2022, **12**, 18373–18396.
37 F. De Vleeschouwer, V. Van Speybroeck, M. Waroquier, P. Geerlings and F. De Proft, *Org. Lett.*, 2007, **9**, 2721–2724.
38 R. G. Parr and W. Yang, *J. Am. Chem. Soc.*, 1984, **106**, 4049–4050.
39 P. P. Zamora, K. Bieger, A. Cuchillo, A. Tello and J. P. Muena, *J. Mol. Struct.*, 2021, **1227**, 129369.
40 C. Fang, S. Wang, H. Xu and Q. Huang, *Sci. Total Environ.*, 2022, **812**, 152455.
41 J. Lee, S. Eom, S. Sohn, T. Kim and K.-D. Zoh, *Chem. Eng. J.*, 2023, **470**, 144041.
42 D. Wang, J. Liang, H. Zhang and J. Zhang, *ACS ES&T Water*, 2022, **2**, 156–164.
43 B. Yang, X. Cheng, Y. Zhang, W. Li, J. Wang and H. Guo, *Environ. Sci. Ecotechnology*, 2021, **8**, 100127.